

Optical properties and remote sensing of coccolithophores

Recent advances and selected applications

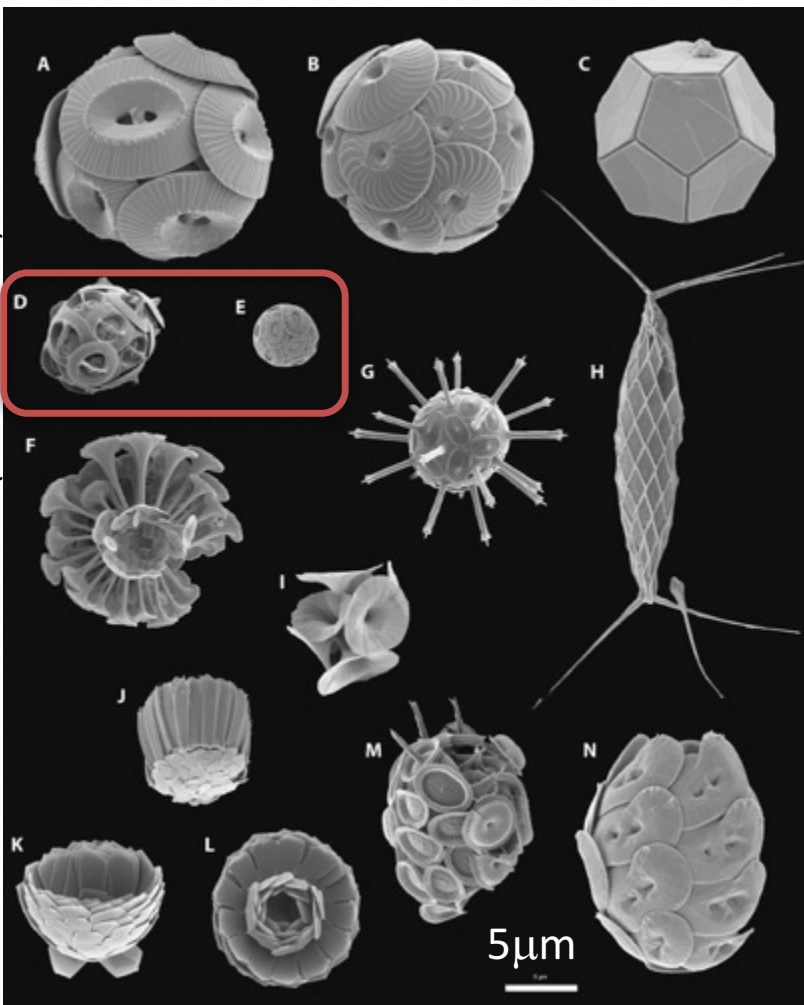
Griet Neukermans

Marie Skłodowska-Curie Postdoctoral Fellow
Laboratoire d'Océanographie de Villefranche-sur-Mer (LOV)
Sorbonne University/CNRS



What are cocolithophores?

Monteiro et al. (2016 – *Sci. Adv.*)



- Calcifying phytoplankton
- Haptophyta; Prymnesiophyceae
- Produce CaCO_3 scales (coccoliths)
- About 200 species, **2 bloom-formers**
- Occur throughout the world ocean
- $5 \mu\text{m} \leq D \leq 40 \mu\text{m}$
- Considered a single PFT
- Comprise about 10% of global phytoplankton biomass
- Major CaCO_3 producers in the open ocean (besides forams and pteropods)

Outline

- OCRS of coccolithophores and their calcite mass (PIC)
 - Quantifying PIC in the ocean + uncertainties
 - Recent advances
 - Caveats of remotely sensed PIC
- Optical properties of coccolithophores
 - (back)Scattering
 - Recent advances
- Applications of optical oceanography in coccolithophore research:
 - Climate change impacts
 - Role in ocean biological carbon sink (calcite ballast effect)

Quantifying PIC in the ocean

Barney Balch
Bigelow (USA)

High latitudes: High PIC, low diversity (blooms dominated by *E. huxleyi*)

Low latitudes: Low PIC, low diversity

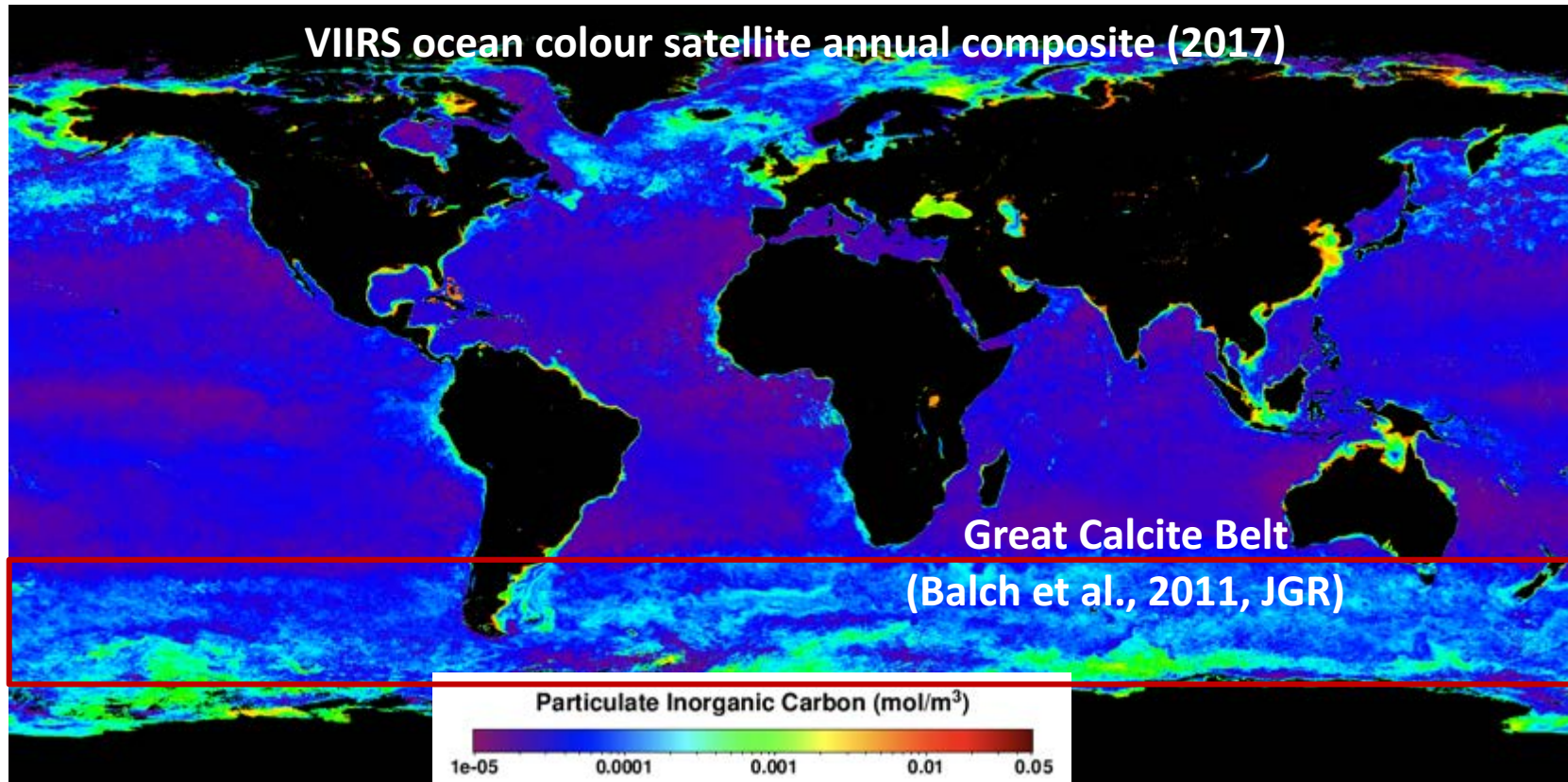
O'Brien et al., 2016 – Progr. Oceanogr.



Global annual coccolithophore bloom coverage of about $2.75 \times 10^6 \text{ km}^2$:

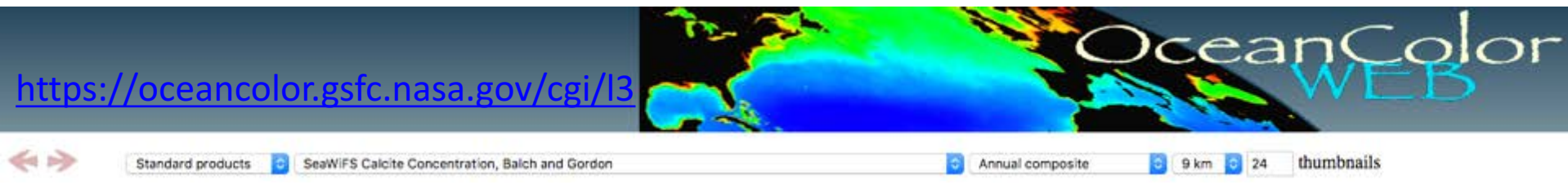
$2 \times 10^6 \text{ km}^2$ in **Southern Hemisphere** and $0.75 \times 10^6 \text{ km}^2$ in Northern Hemisphere.

Moore et al., 2012 – RSE



NASA's standard PIC algorithm

“Balch and Gordon”



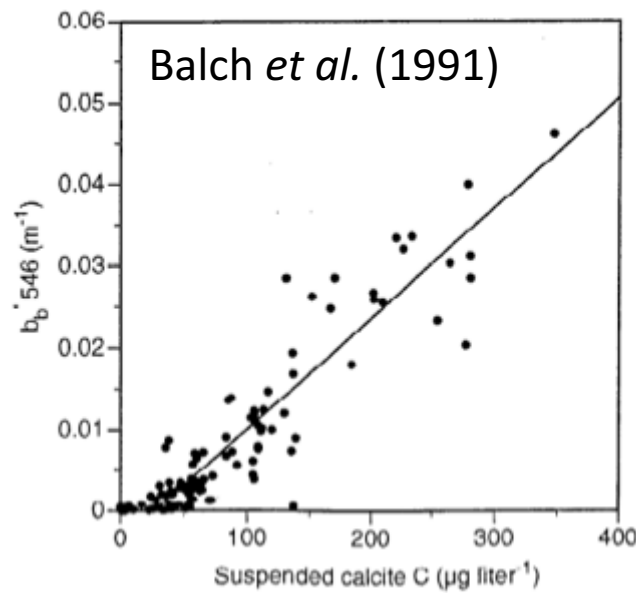
a **hybrid** algorithm, switching between:

The 2-band approach of Balch *et al.* (2005) for Low-Medium PIC or
The 3-band approach of Gordon *et al.* (2001) for high PIC

The 2-band approach is applied, unless PIC > 40 µg PIC/L or 3 mmol C/m³;
then the 3-band algorithm is used.

The “Balch and Gordon” algorithm is **applicable to all current ocean color sensors**.

Algorithm **calibration** in Maine waters and in UK waters (*E. huxleyi* dominated).
Mainly **validated** in Maine waters and high latitude oceans and seas.



PIc algorithm for high PIC

Gordon *et al.* (2001)

Heart of the algorithm:

$$b_{bpic}(546 \text{ nm}) = 1.6 \times [\text{PIC in mol m}^{-3}] - 0.0036$$

$$b_{bpic}(\lambda) = b_{bpic}(546) \times (546/\lambda)^{1.35}$$

[Based on in situ measurements by Balch *et al.* (1991)]

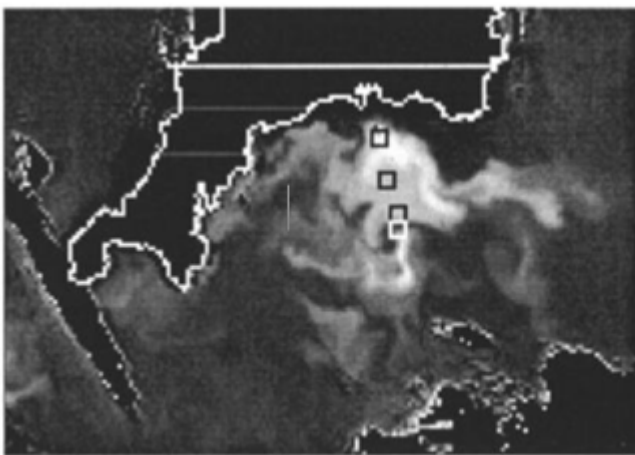


Figure 1. $b_b(546)$ in m^{-1} retrieved from the July 30, 1999 SeaWiFS image of Plymouth, UK. Areas of enhanced backscat-

3-band algorithm retrieving $b_b(546 \text{ nm})$ from SeaWiFS reflectance in Red and NIR bands (670, 765, 865nm)

Assumptions:

- $\rho_w(765, 865\text{nm})=0$ to get $\rho_w(670\text{nm})$
- $\rho_w(\lambda)=b_b(\lambda)/(6(a_w(\lambda)+b_b(\lambda)))$ with $\lambda=670\text{nm}$

Suitable for high concentrations of CaCO_3 , when B-G bands often saturate (not accurate for PIC concentrations $< 3 \text{ mmol m}^{-3}$)

maximum RMS error of the algorithm is $\pm 15 \mu\text{g/L}$ (or 1.2 mmol m^{-3})
= about 5-10% of PIC in dense bloom (Balch, 2004)

PIC algorithm for low-med PIC

Balch *et al.* (2005)

Heart of the algorithm (same as Gordon algo):

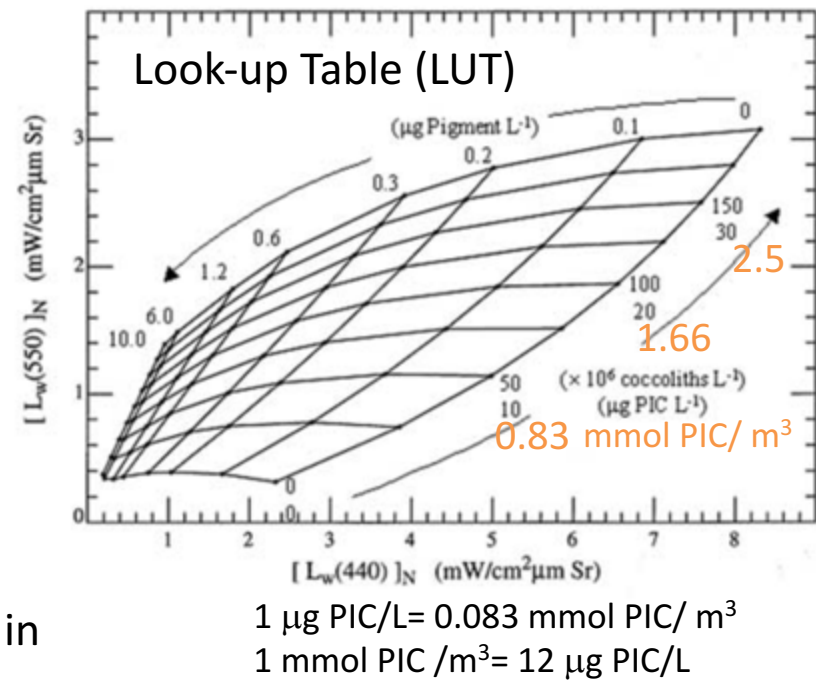
$$b_{\text{bpic}}(546 \text{ nm}) = 1.6 \times [\text{PIC in mol m}^{-3}] - 0.0036$$

$$b_{\text{bpic}}(\lambda) = b_{\text{bpic}}(546) \times (546/\lambda)^{1.35}$$

PIC is retrieved from a LUT based on semi-analytical OCRS model of Gordon *et al.* (1988)

Validated with in situ data of b_{bpic} , PIC, Chla, and L_w mainly in Maine waters (*Ehux* dominated)

Retrieval **uncertainty**: due to natural variability in phytoplankton-detritus b_b corresponds to
 $25 \times 10^6 \text{ coccoliths/L} = 5 \mu\text{g PIC/L} = 0.41 \text{ mmol PIC/m}^3$



Major limitations:

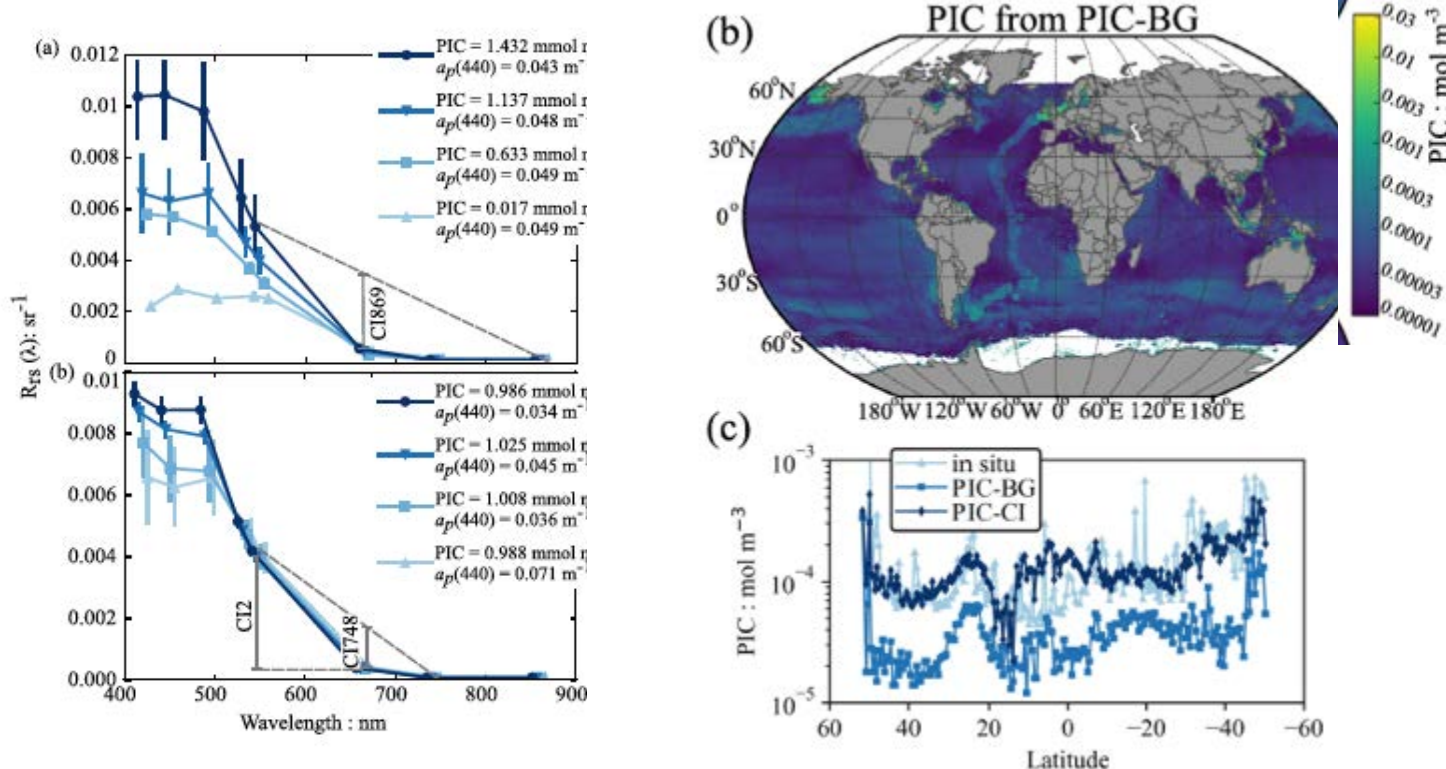
- dependency on the reflectance model (assumed constant phyto-detritus b_b)
- Estimate of “excess backscatter” -> particles other than PIC may also cause excess backscatter
- absolute radiance -> sensitivity to atmospheric correction errors

Alternative PIC algorithm

Referred to as calcite_CI2, status=test

Mitchell *et al.* (2017)

Reflectance difference approach, inspired by Hu *et al.* (2012) for Chla



Color index using 547 and 667 nm, denoted CI2

$$\text{CI2} = R_{rs}(547) - R_{rs}(667)$$

More **resistant** to atmospheric correction errors and residual errors in sun glint corrections than the Balch *et al.* (2005) algorithm.

Potential to replace the Balch *et al.* (2005) algorithm currently being investigated

PICT algorithm caveats

False positives for high PIC (highly reflective waters) produced by:

- Whitings = patches of suspended fine-grained calcium carbonate



Bahamas Banks



<https://earthobservatory.nasa.gov/>

(Dierssen et al., 2009 – Biogeosciences)

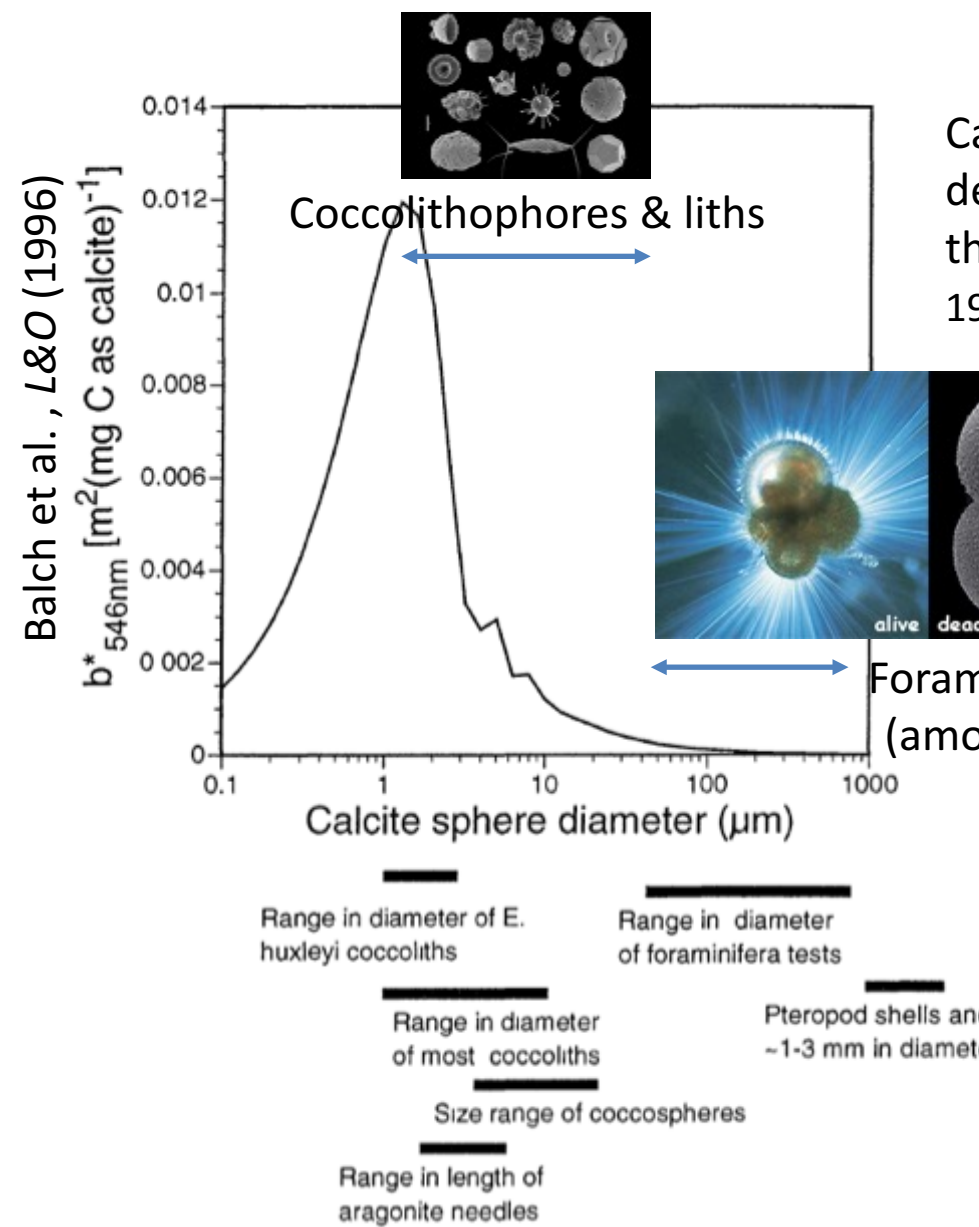


(e.g., Dierssen et al., 2002).

- Glacial rock flour in some high-altitude lakes
- High concentrations of empty diatom frustules (e.g. on shallow shelves, Broerse et al., 2003) or suspended sediments
- In polar waters: Floating sea-ice
- Bubbles
- Phaeocystis foam

(See Balch, 2018, Ann. Rev. Mar. Sci. or Tyrrell and Merico, 2004)

Light scattering properties of CaCO_3 particles in the ocean



Calcite-specific scattering coefficient is size-dependent according to anomalous diffraction theory for non-absorbing spheres (Van de Hulst, 1981).

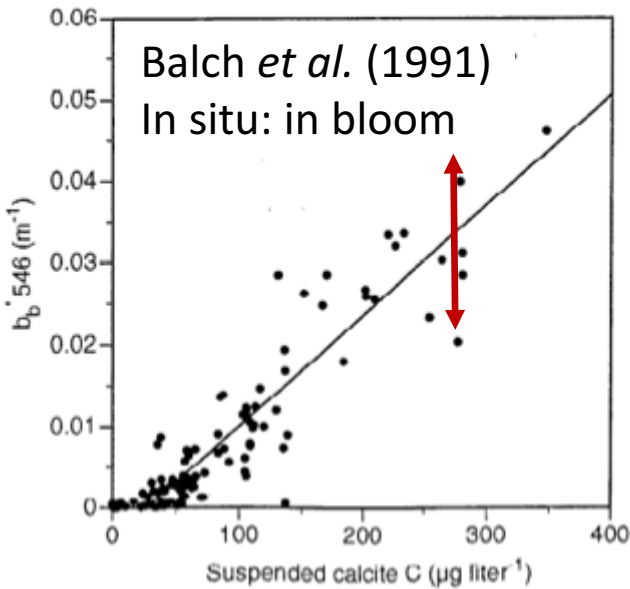


Negligible contribution from larger calcite particles (forams and pteropods) to b_b and thus to R_{rs}



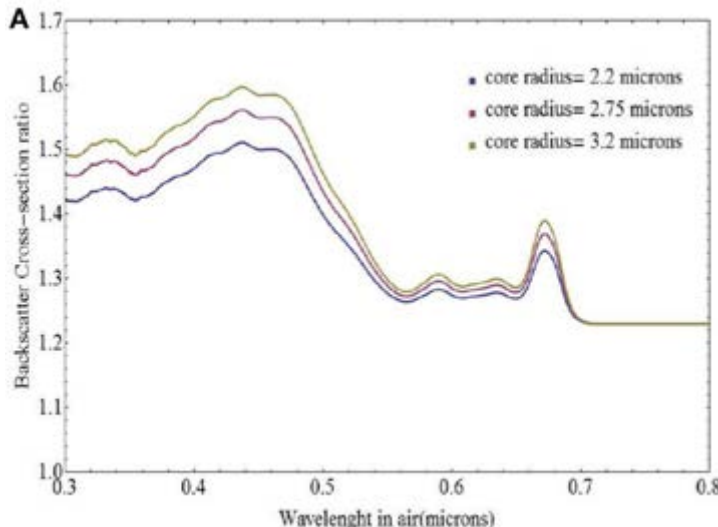
Pteropods (1-3mm)
"sea snails"

Light backscattering vs. PIC



Heart of NASA's PIC algorithm :
 $b_{\text{bpic}}/\text{PIC} = \text{constant}$

Variability in $b_{\text{bpic}}/\text{PIC}$ due to
coccolith detachment?

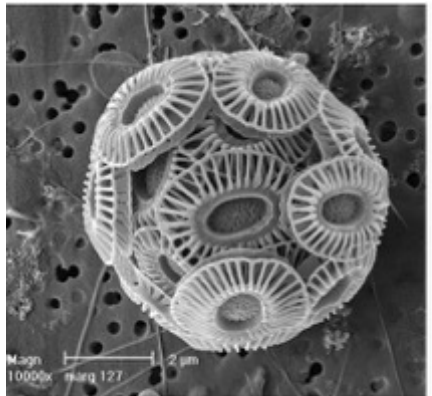


Optical modeling studies show that $b_{\text{bpic}}/\text{PIC}$ does NOT depend much on whether coccoliths are attached to or freed from the coccospHERE

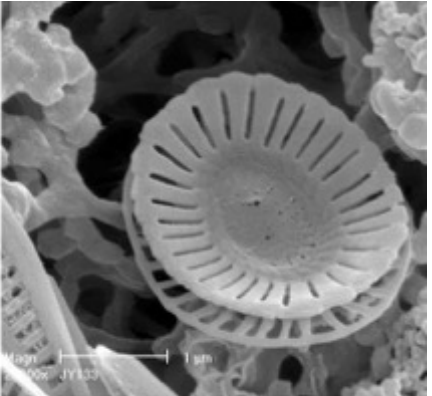
(see also Gordon *et al.*, 2009, Appl. Opt.)

Spectral backscattering properties of *E.huxleyi*

Strongly depend on coccolith morphology (and size, indirectly)

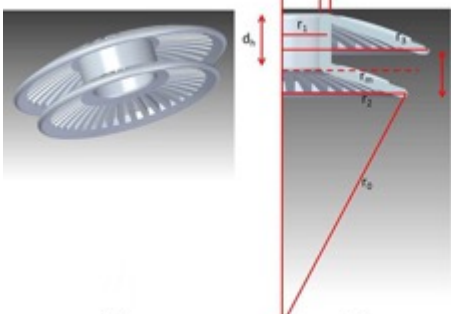


coccospHERE



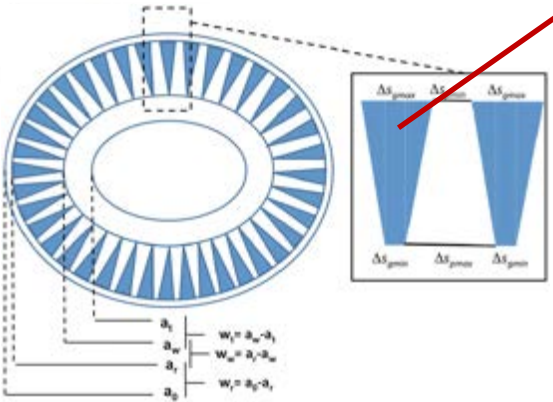
coccolith

SEM of *E. huxleyi* (J. Young)



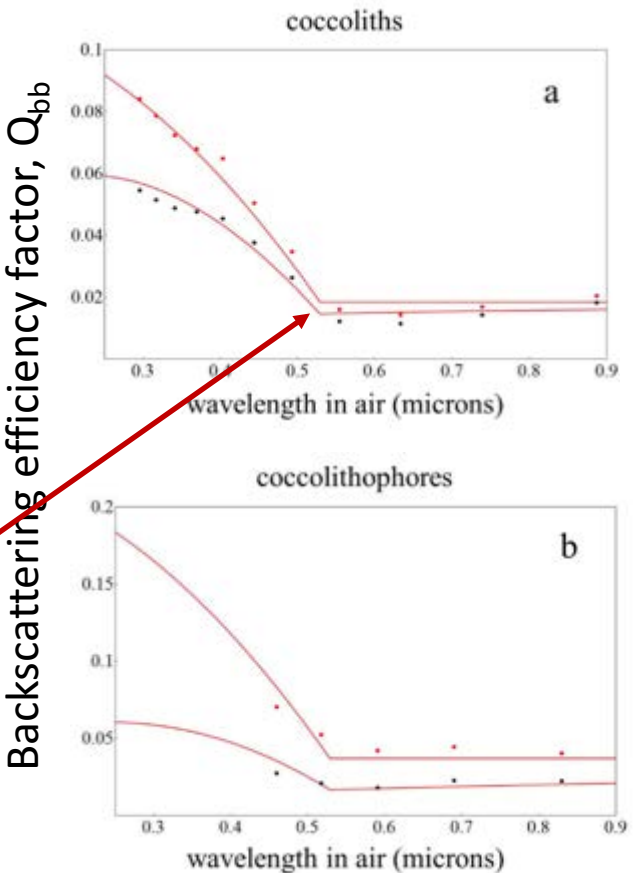
(a)

(b)

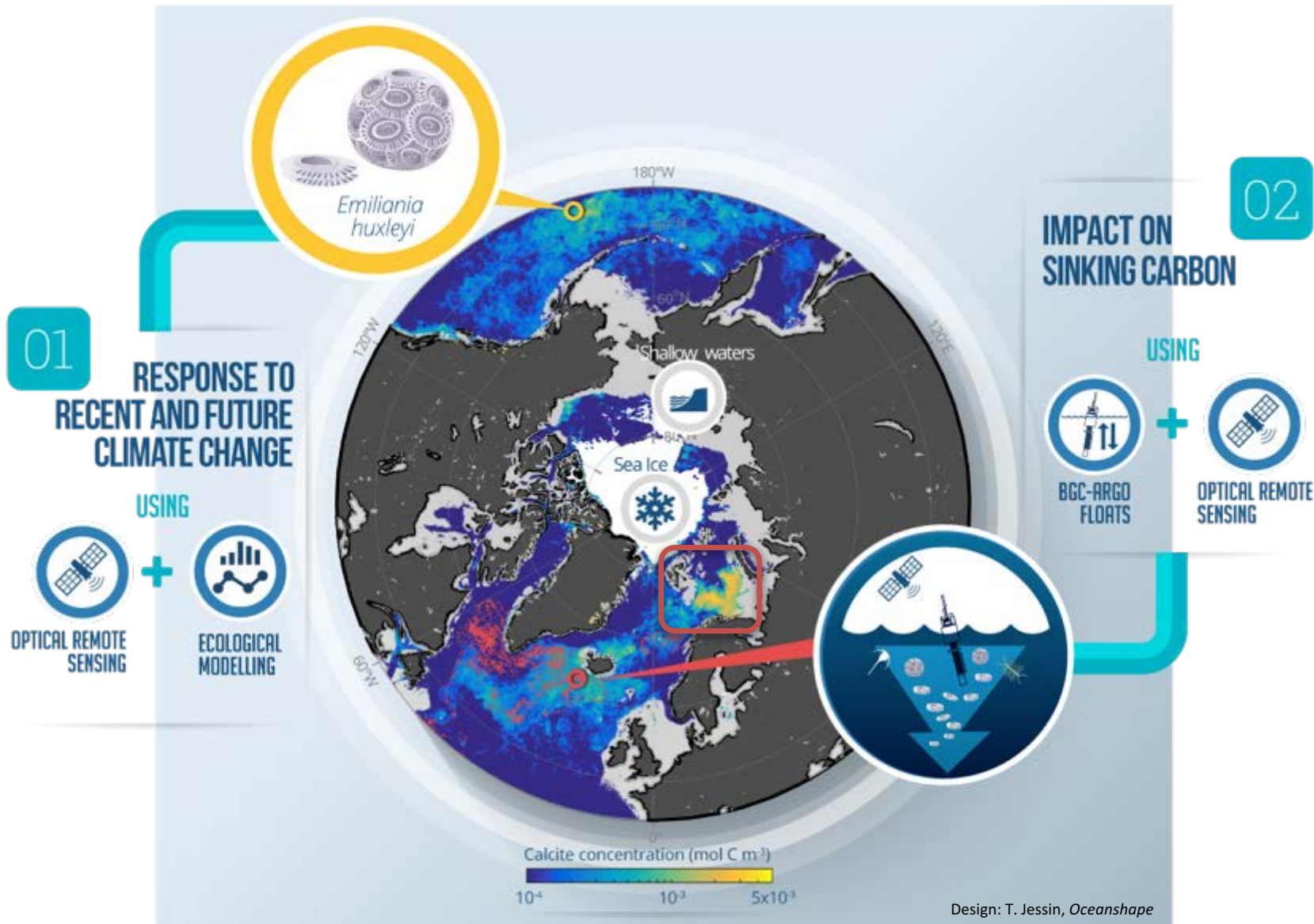


Model of *E. huxleyi* coccolith

(Fournier and Neukermans, 2017, Opt. Expr.; Neukermans and Fournier, 2018, F.Mar.Sci.)

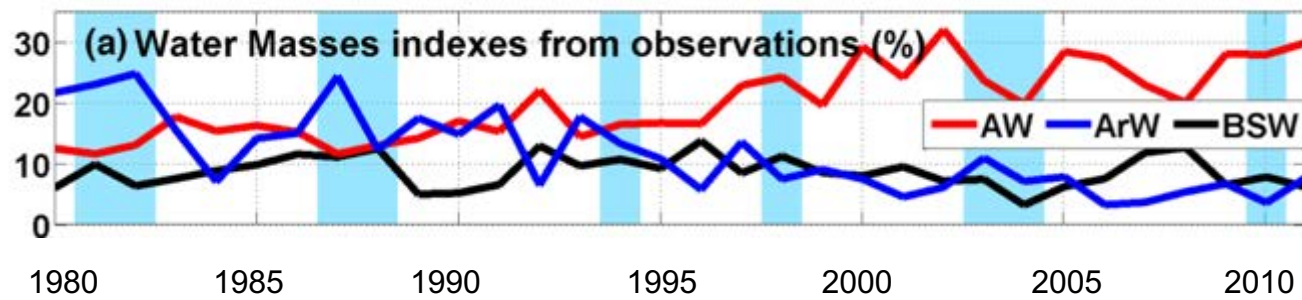
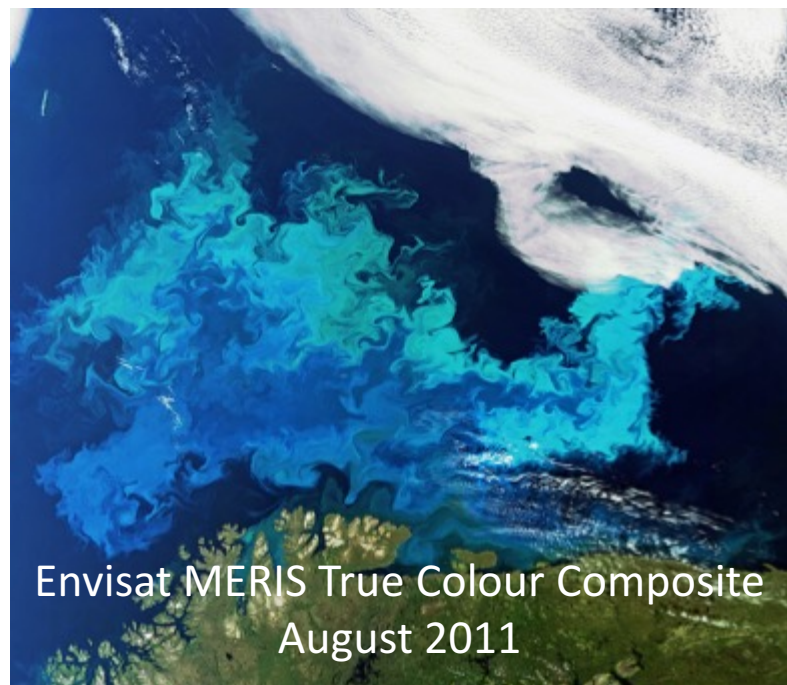
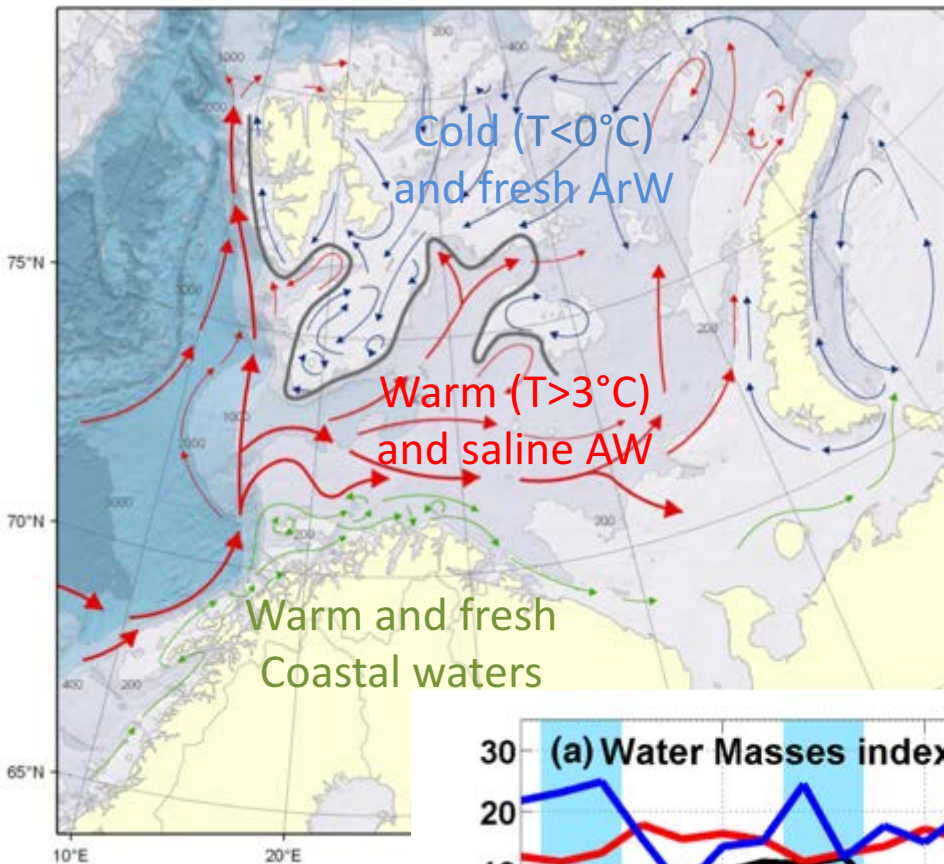


Selected applications: WhiteShift project



RESPONSE TO CLIMATE CHANGE

A case study in the Barents Sea (70° - 80° N)



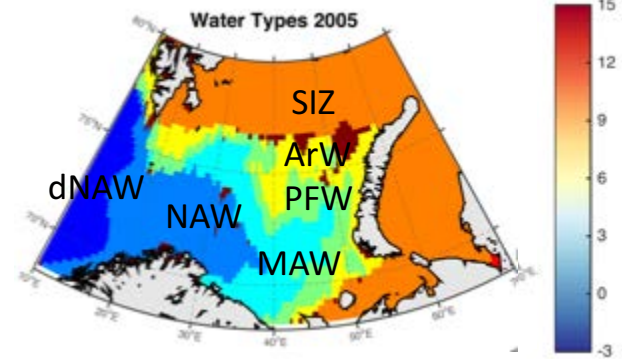
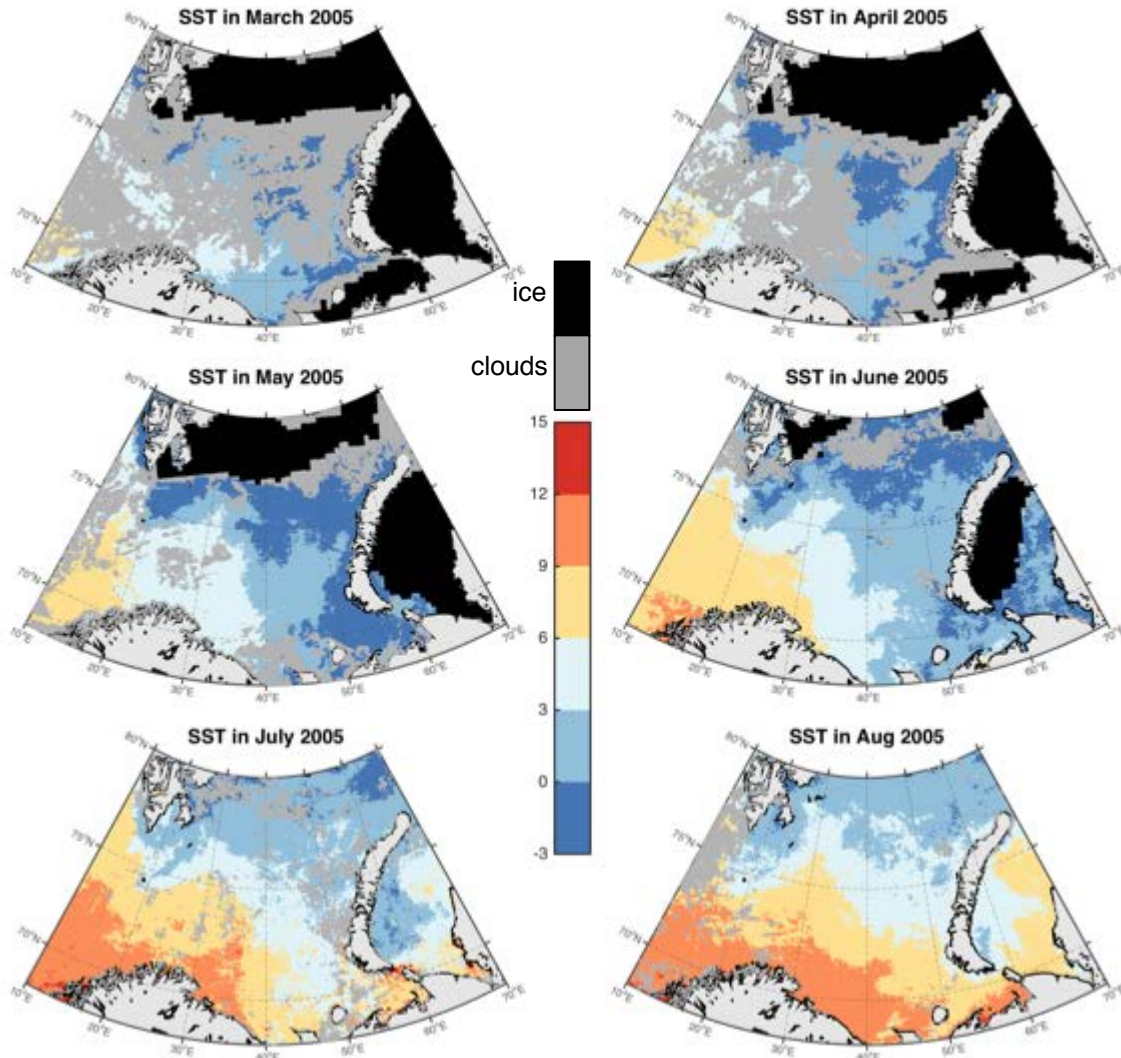
Atlantic Water volume tripled → **Atlantification** (Arthun *et al.*, 2012 – *J. Clim.*)

“increase in Atlantic heat transport due to both strengthening and warming of the inflow”

Space-based water mass classification

Example 2005: SST from AVHRR, Sea ice from SSMI

$$-0.49C < T(PFW) < 0.62C$$



(d) NAW: $SST > 3C$ (Loeng, 1991)

MAW: $PFW_u < SST < 3C$

PFW: $PFW_l < SST < PFW_u$

ArW: $SST < PFW_l$

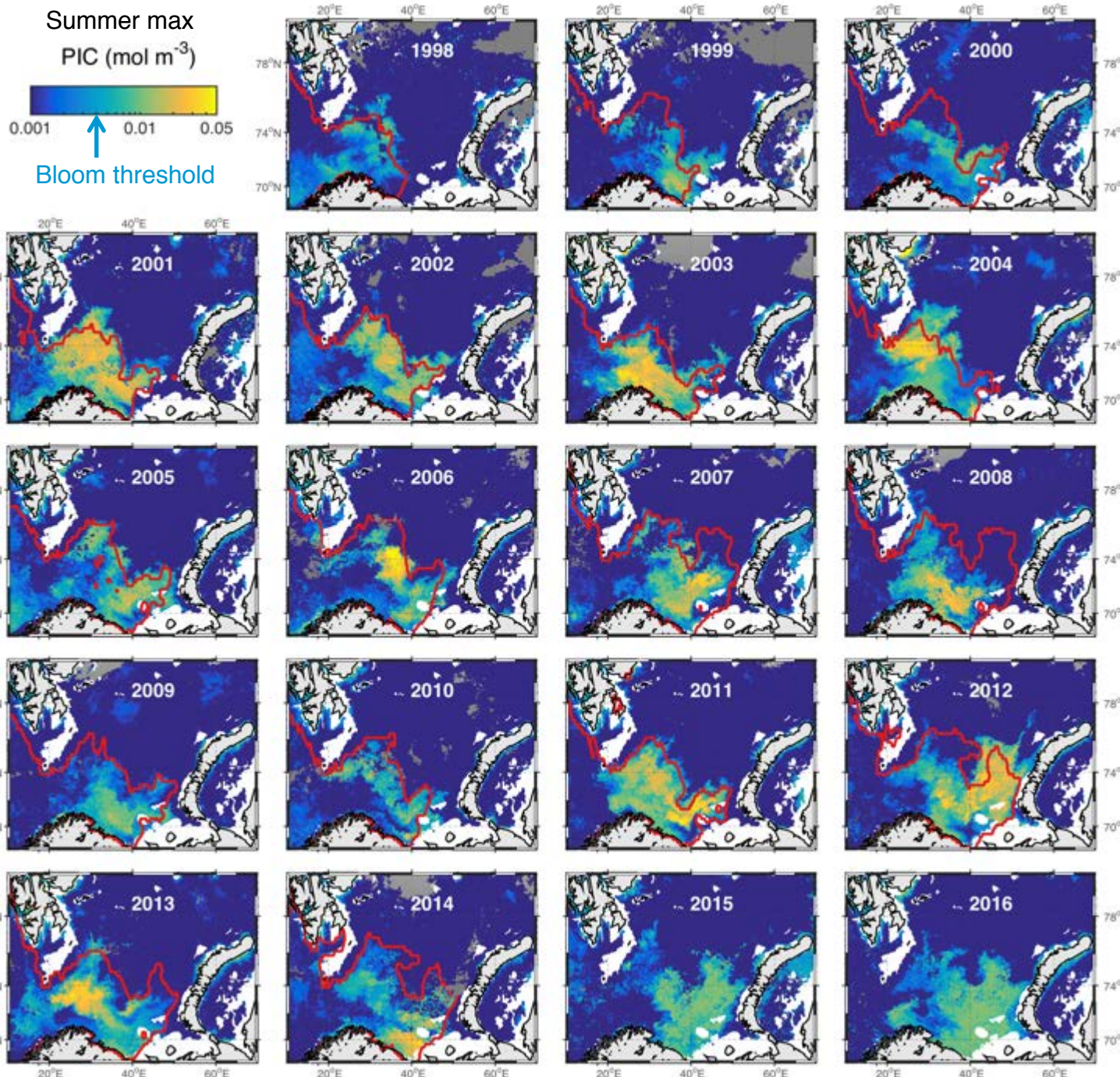
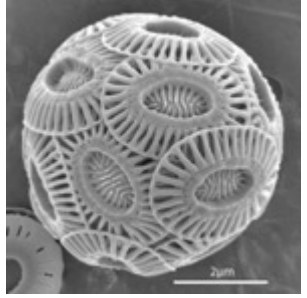
SIZ: seasonally ice-covered

U: Unclassified (no SST)

Classification successfully validated with hydrographic dataset of Oziel et al. (2016)

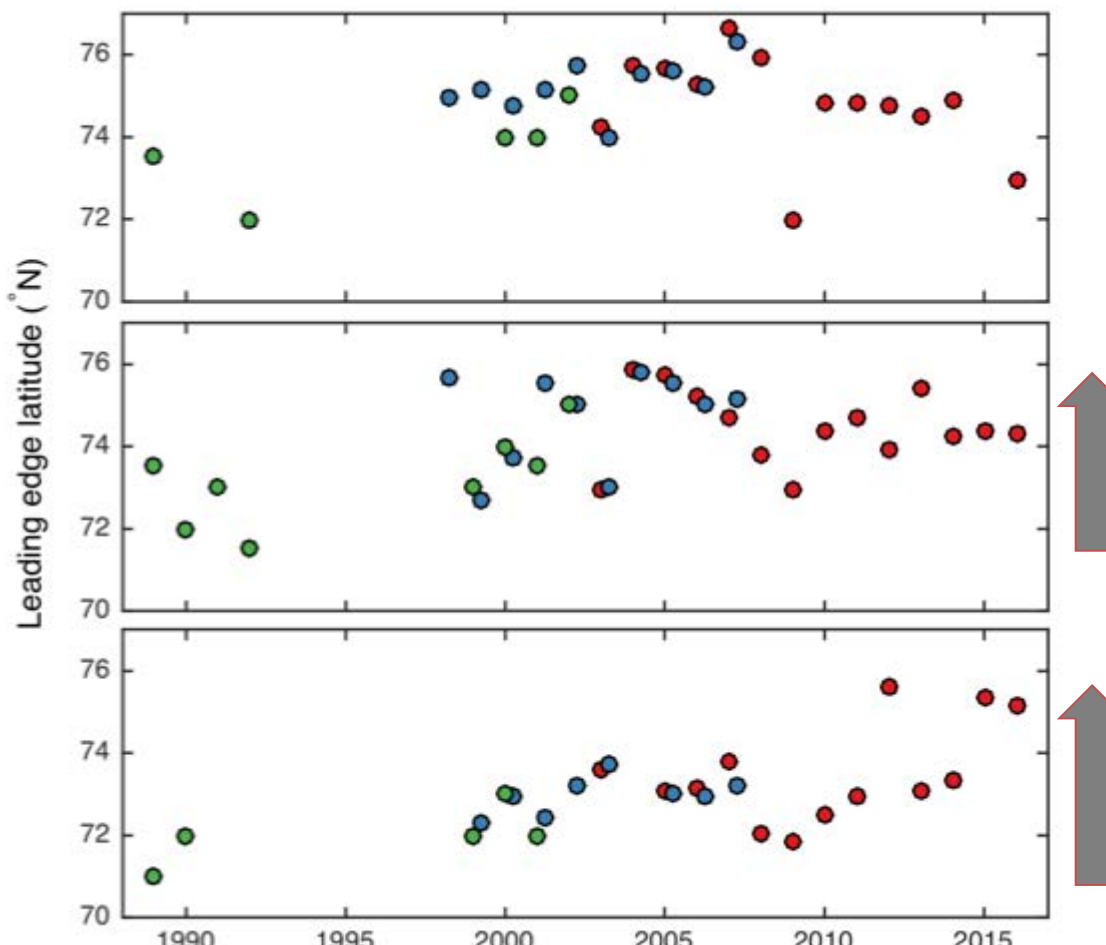
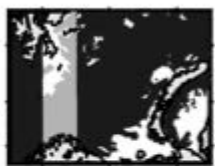
Interannual variability in extent of *E. huxleyi* blooms

and Atlantic waters



Poleward expansion of *E. huxleyi* blooms

a



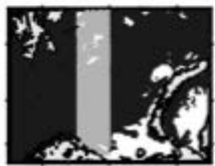
n.s.

n.s.

390 km
(1989-2016)

501 km
(1989-2016)
56 km/yr
(2010-2016)

b



c

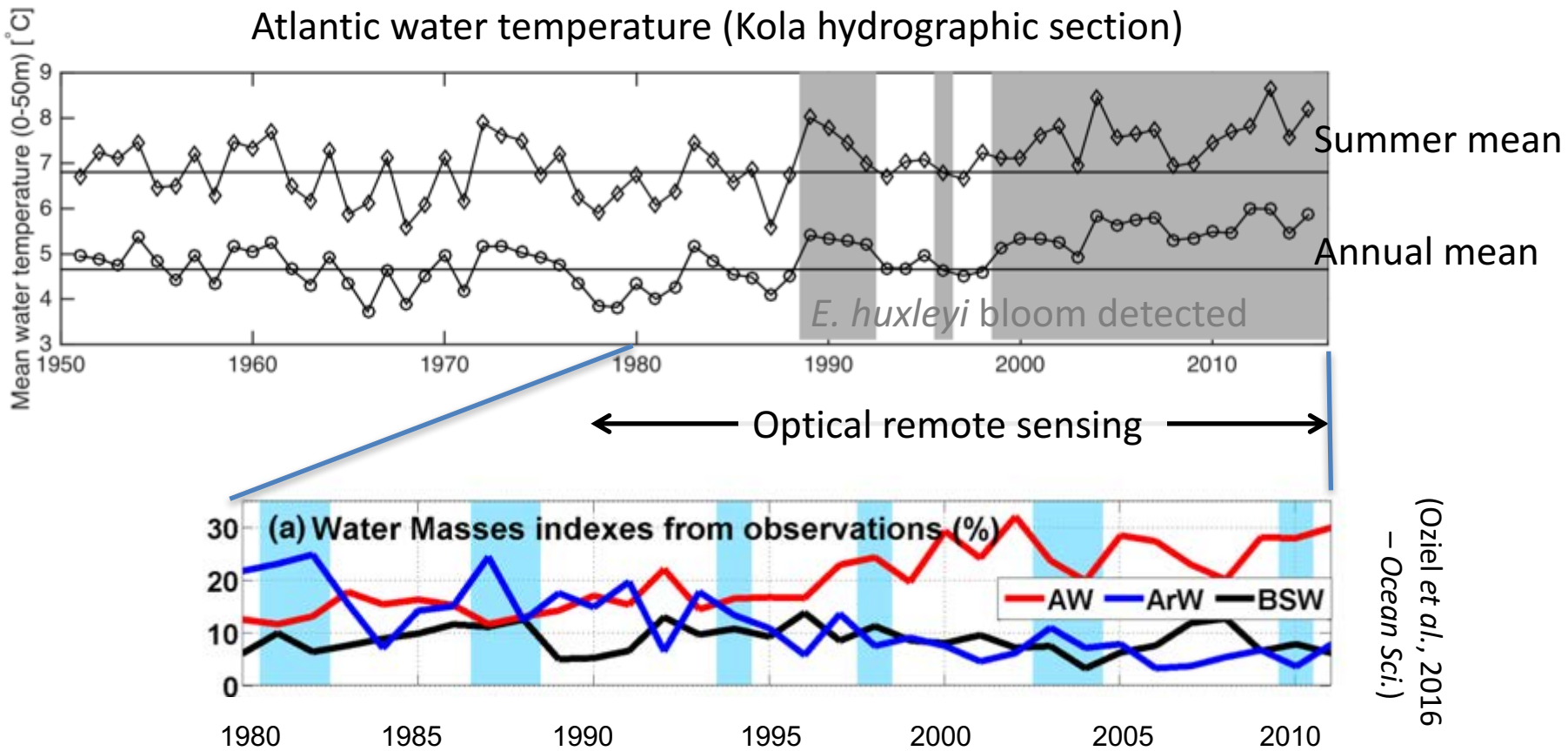


Smyth *et al.* (2004 – *Geophys. Res. Lett.*)

Loveday and Smyth (2018 – *ESSD*)

AVHRR →
← SeaWiFS →
← MODIS →

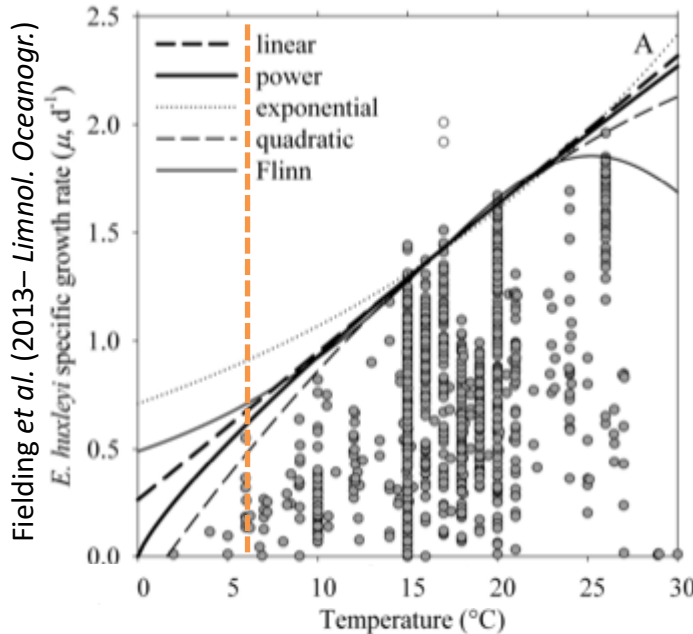
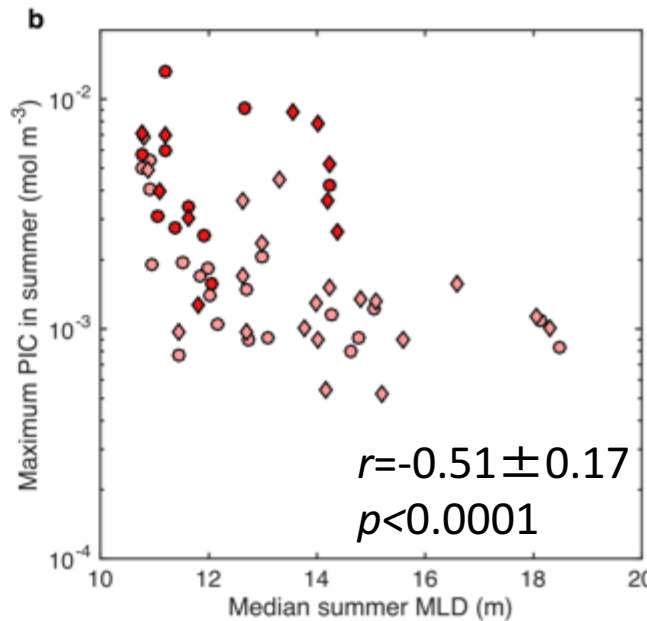
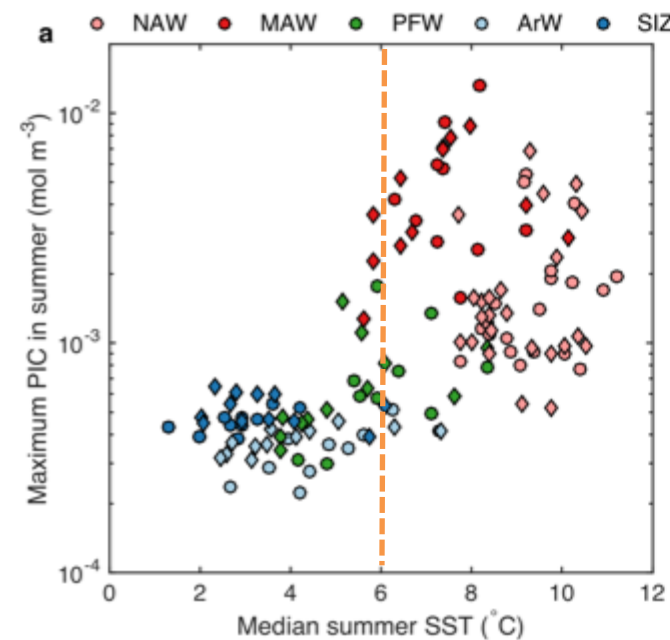
Poleward expansion of *E. huxleyi* blooms



Atlantic Water volume tripled → *Atlantification* (Arthun et al., 2012 – *J. Clim.*)

Poleward expansion in the Barents Sea is driven by increased intrusion and warming of Atlantic waters

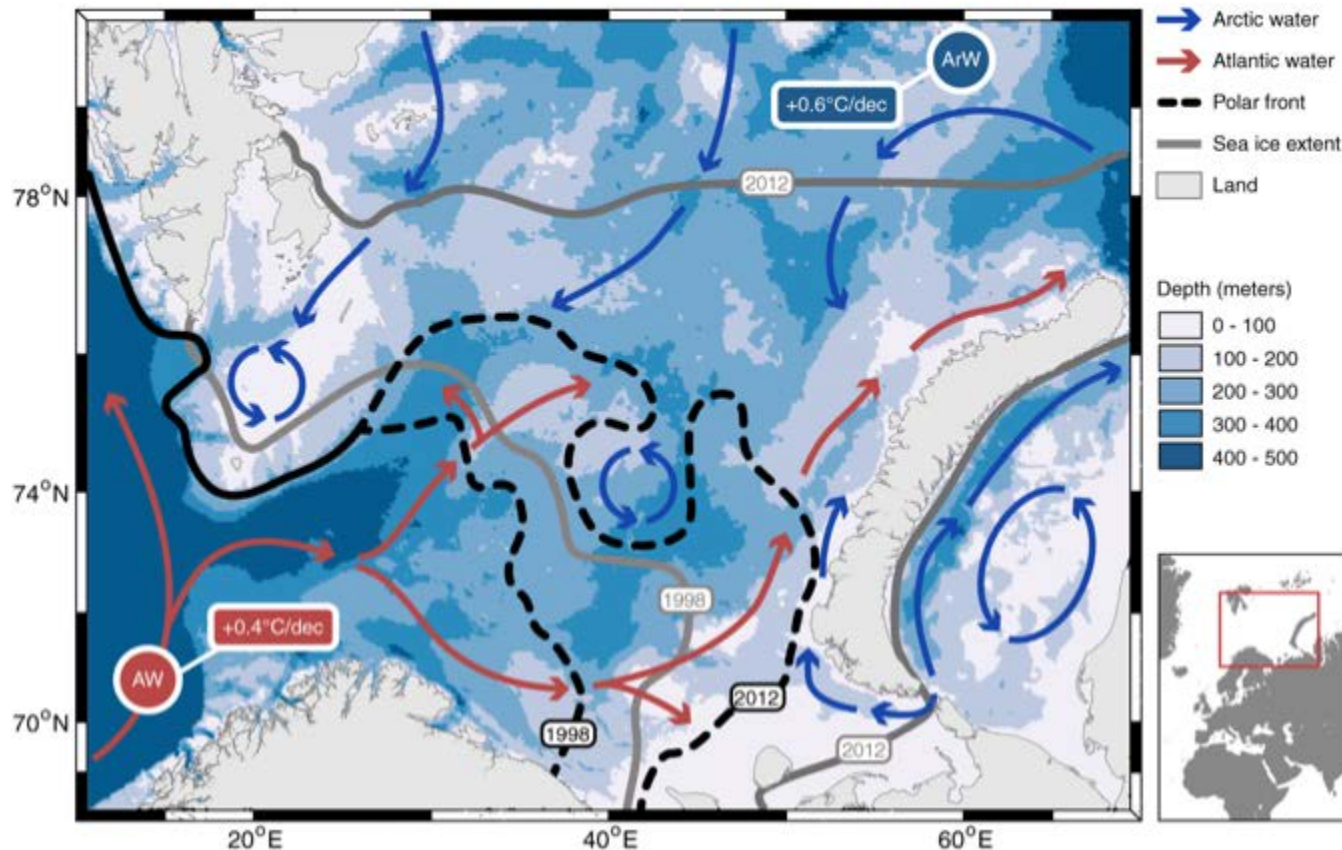
E. huxleyi blooms – environmental drivers



E. huxleyi requires $T>6\text{C}$ in order to form blooms

MLD between 10 and 20m are known to favor *E. huxleyi* blooms (Nanninga and Tyrell, 1996)

Will *E. huxleyi* blooms continue to expand poleward?

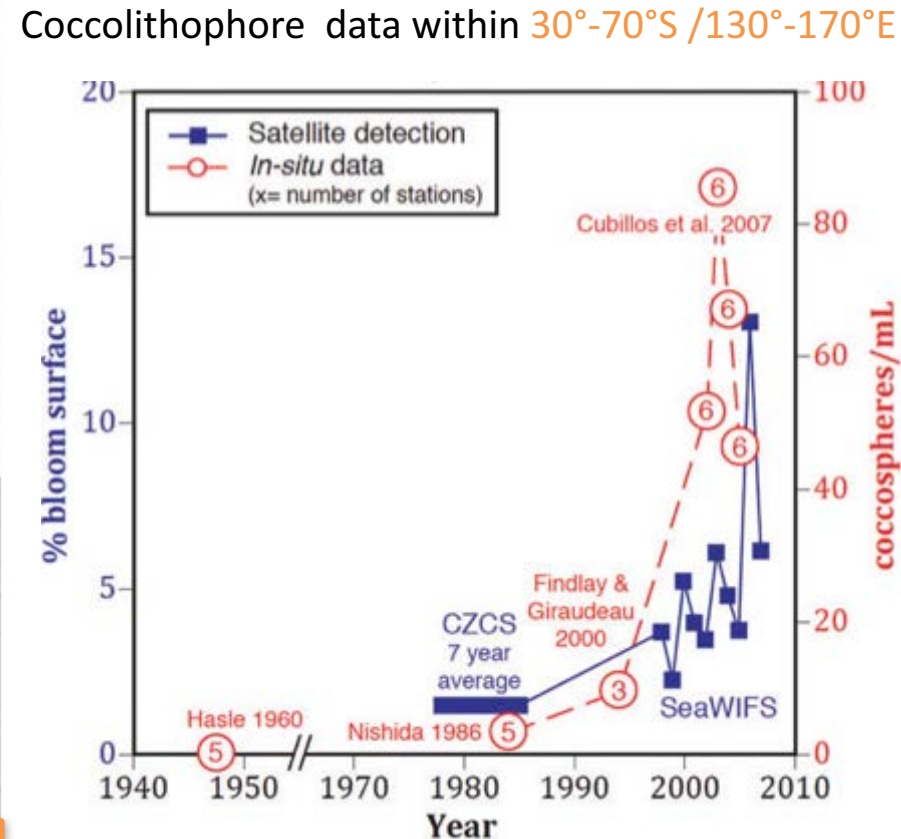
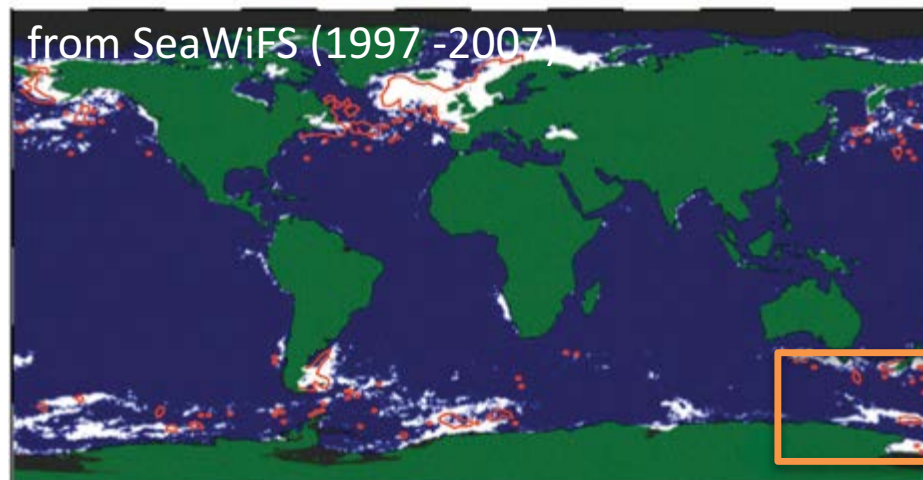
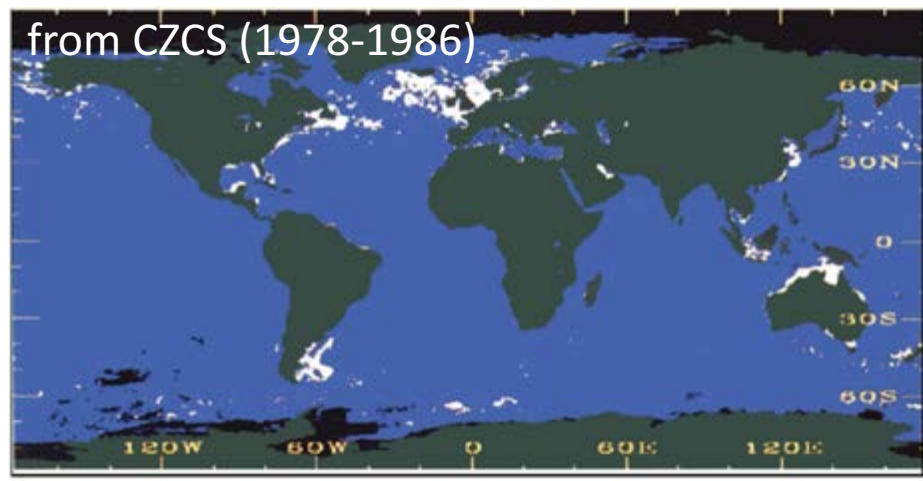


- + Self-amplifying feedback loop promotes further atlantification (Smedsrød *et al.*, 2013)
- + T is rising faster in ArW than in AW → weakening of polar front in next century
- + Nutrients in Atlantic waters are declining: Silicates faster than Nitrates, 20% vs. 7% in 1990-2010 (Rey, 2012) → favorable for non-silicifying phytoplankton
- Deepening of Mixed layer trend since 1979 (Peralta-Ferriz and Woodgate, 2015; Oziel *et al.*, 2017)

Poleward expansion of *E. huxleyi*

A global phenomenon? Proposed by Winter *et al.* (2014 – *J. Plankton Res.*), based on OCRS (CZCS and SeaWiFS) and in situ data.

Climatology of classified coccolithophore blooms

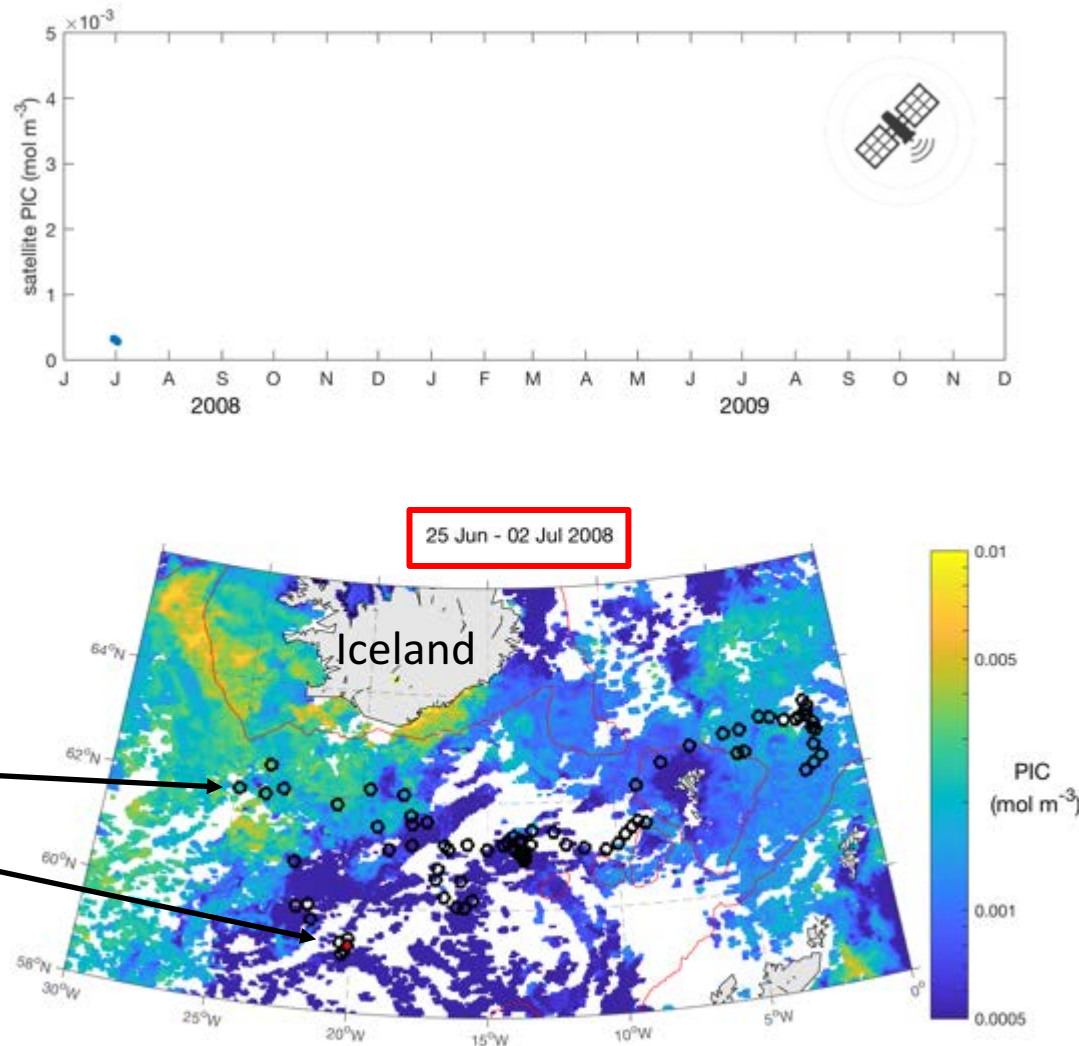
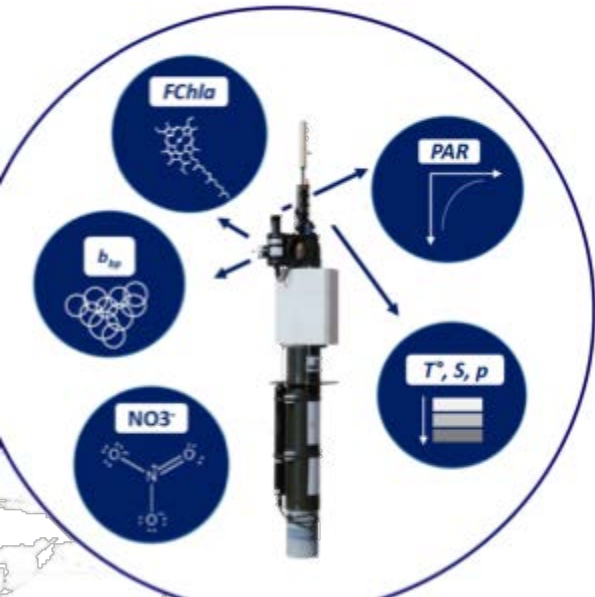


Bloom size and intensity increased in the 1990s. Why?

02

IMPACT ON SINKING CARBON

A case study in the Irminger Sea

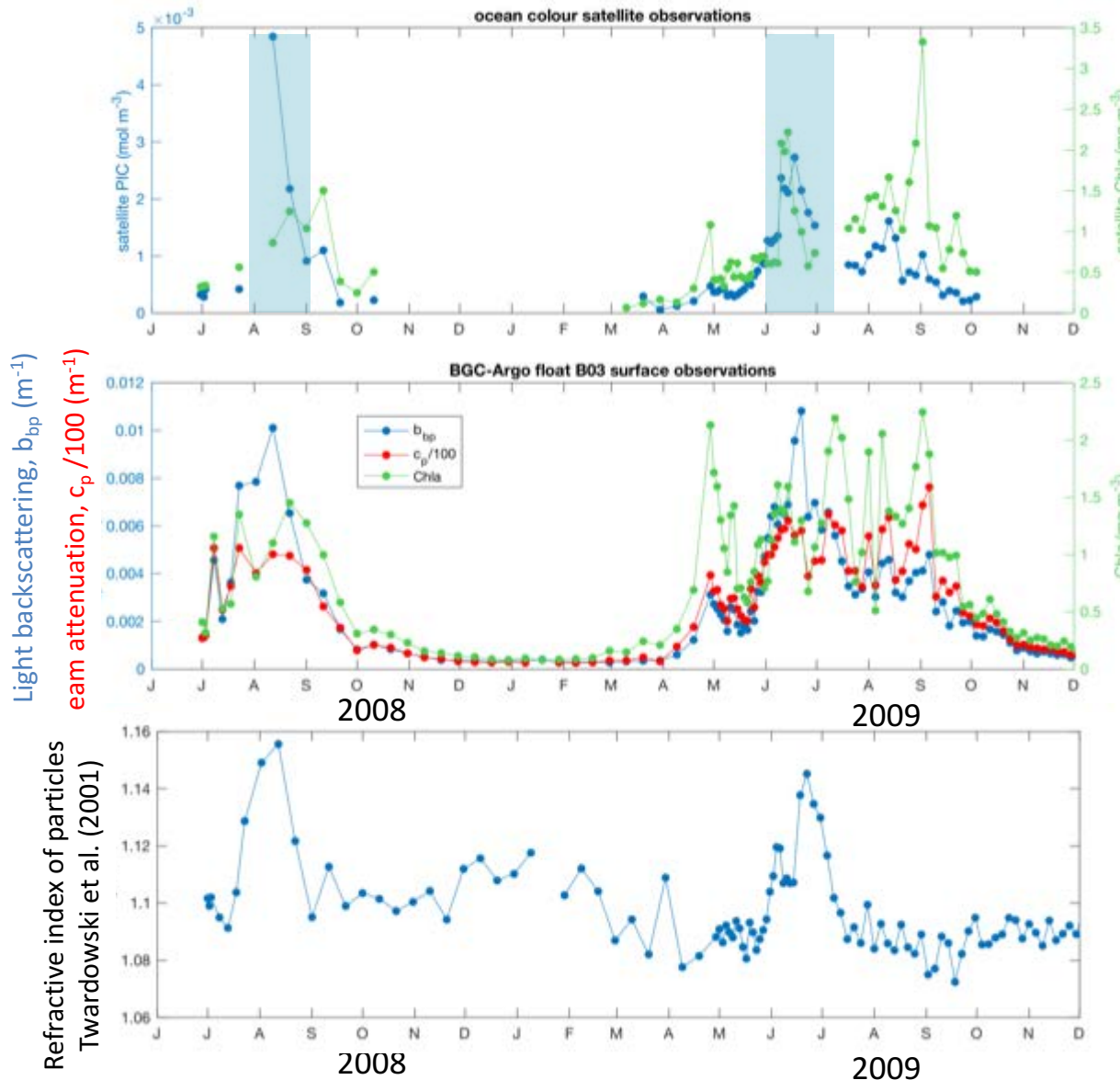


Profiles on float trajectory
Current float position

02

IMPACT ON SINKING CARBON

A case study in the Irminger Sea



Future work: Brittany *E. huxleyi* bloom monitoring

Objective: Monitoring biogeochemistry of an *E. huxleyi* bloom off the coast of Brittany in April-June 2019

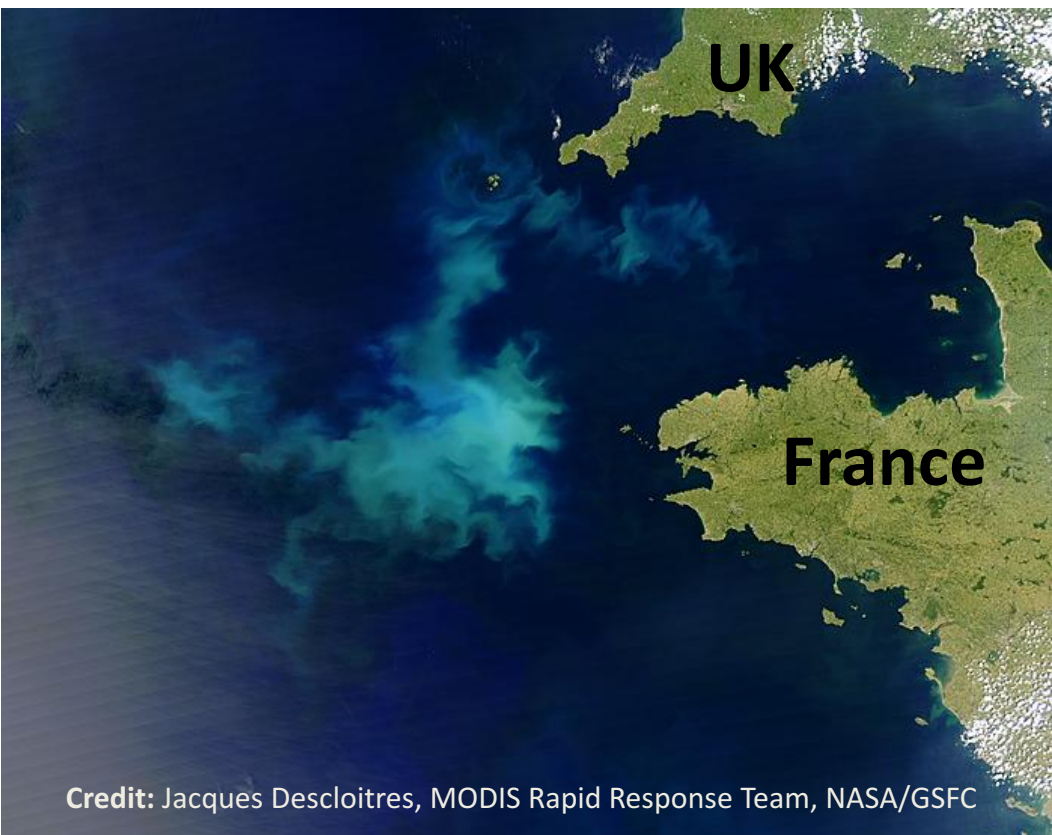
Sampling platforms:



IODYSSEUS and TARA

<https://www.iodysseus.org/>

+



Credit: Jacques Descloitres, MODIS Rapid Response Team, NASA/GSFC

Optics:

- backscattering
- Hyperspectral absorption and scattering
- Chla + CDOM fluorescence
- Particle size (LISST-100X)

Discrete samples:

POC, PIC, HPLC

Biogeochemistry:

- in-water pCO₂
- Carbon export from BGC-Argo float

Aerosols

Collaborators: Roscoff, UMaine, ICCF, Weizmann Institute, ...

A satellite image of the Arctic Ocean. The upper half shows dark blue and black areas representing open water or thin sea ice. The lower half shows a large, bright cyan-colored area representing a phytoplankton bloom. In the bottom right corner, there is a green and brown landmass with a river system flowing into the ocean.

Thank you!